Viscous Shock Layer at the Stagnation Point with Nonequilibrium Air Chemistry

F. G. BLOTTNER*
Sandia Laboratories, Albuquerque, N.Mex.

A finite-difference method and a nonlinear overrelaxation method are investigated for solving the viscous shock layer at the stagnation point of a blunt body. An air gas model is employed with finite reaction rates and accurate thermodynamic and transport properties. For a body with a 1-in. nose radius and at a velocity of 20 kfps, the present results at 100, 150, 200, and 250 kft show that boundary-layer theory with the inviscid edge flow in chemical equilibrium is appropriate for some altitude below 150 kft. When the altitude is 250 kft, the effects of shock slip must be included in the viscous shock-layer solution. For this case, the air is only slightly dissociated and ionized. The present results, with a seven-species air model, are in general agreement with the diatomic air model results of Cheng and Chung.

Nomenclature

c_i = mass fraction of species i, ρ_i/ρ
c_{pi} = specific heat at constant pressure of species i, ft²/(sec² °R)
$\bar{c}_p$ = frozen specific heat at constant pressure of the mixture, $\sum_i c_i c_{pi}$, ft²/(sec² °R)
D_{ij} = multicomponent diffusion coefficient, ft²/sec
$\mathfrak{D}_{ij}$ = binary diffusion coefficient, ft²/sec
f' = velocity ratio, u/u_e
h = enthalpy, $\sum_i h_i c_i$, ft²/sec²
h_i = enthalpy of species i, ft²/sec²
j_i = mass flux relative to the mass-average velocity, slug/(ft²-sec)
k = thermal conductivity of mixture, lb/(sec °R)
k_{fr}, k_{br} = forward and backward rate constants
l = density-viscosity product, $\rho\mu/(\rho\mu)_r$
L_{ij} = multicomponent Lewis-Semenov number, $\bar{c}_p \rho D_{ij}/k$
$\mathfrak{L}_{ij}$ = binary Lewis-Semenov number, $\bar{c}_p \rho \mathfrak{D}_{ij}/k$
M = molecular weight of the mixture, $1/(\sum_i c_i/M_i)$, lb/lb-mole
M_i = molecular weight of species i, lb/lb-mole
NI = number of chemical species
Pr = Prandtl number, $\bar{c}_p\mu/k$
p = pressure, lb/ft²
R = universal gas constant, lb ft²/(lb-mole sec² °R)
R_N = nose radius, ft
Re_s = shock Reynolds number, $\rho_\infty V_\infty R_N/\mu_s$
r = distance from axis in axisymmetric problems, ft
T = temperature, °R
T_K = temperature, °K
u,v = velocity components tangential and normal to body surface, ft/sec
V = transformed normal velocity (Eq. 3a)
V_∞ = freestream velocity, fps
w_i = mass rate of formation of species i, lb sec²/(ft⁴ sec)
x = distance along surface from leading edge or stagnation point, ft
y = distance along normal from surface, ft
ϵ = density ratio across shock, ρ_∞/ρ_s
η = transformed y coordinate
ξ = transformed x coordinate, lb² sec²/ft^{2(2−j)}
$\Delta\eta, \Delta\xi$ = step sizes in transformed coordinates
θ = temperature ratio, T/T_e
κ_c = curvature of body, 1/ft
μ = viscosity, lb sec/ft²
ρ = density, lb sec²/ft⁴
ρ_i = density of species i, lb sec²/ft⁴
Δ = shock standoff distance, ft

Subscripts

b,w = conditions at body surface
e = conditions at outer edge of shock layer or boundary layer
r = quantities evaluated at some reference condition
s = conditions behind shock wave
∞ = freestream conditions

Superscripts

j = 0,1 two-dimensional, axisymmetric body

Presented at the AGARD Seminar on Numerical Methods for Viscous Flows, National Physical Laboratory, Teddington, England, September 18–21, 1967; received March 10, 1969; revision received August 15, 1969. The author wishes to express his appreciation to M. Johnson of Computer Applications Inc. for writing the computer program and for assistance in obtaining the numerical results presented in this paper. This work was supported by the United States Atomic Energy Commission.

* Staff Member, Aerothermodynamic Research Department. Member AIAA.

1. Introduction

AT the stagnation point of a blunt body, the Navier-Stokes equations can be reduced to ordinary differential equations with two-point boundary conditions. This problem is often considered easier to solve than the partial differential equations for a thin shock layer or a boundary-layer flow around the body. However, for flows with many chemical species and fast reaction rates, the ordinary differential equation can be exceedingly difficult to solve. Also, to start the solution of the partial differential equations, the stagnation-point ordinary differential equations must be solved to provide initial profiles of the dependent variables. The solution of the same type of ordinary differential equations occurs for initial profiles for boundary-layer flows at the tip of a sharp body such as a cone or wedge.

The purpose of this paper is to investigate and develop techniques for solving the viscous shock-layer flow at the stagnation point of a blunt body for air with chemical reactions occurring at finite rate. At the same time, the solution for boundary-layer flows at a stagnation point, or a tip of a cone or wedge, will be considered. In the problems of interest, there can occur many chemical species as a result of the dissociation of air and the ablation products. Initial profiles at the tip of a sharp body are the easiest to obtain, as the term involving the chemical production term is zero and the governing equations are the same as those for chemically frozen flow. The initial profiles at a stagnation point with finite rates are exceedingly difficult to obtain, being similar to the problems encountered in obtaining locally similar solutions along a wall.[1] Two techniques for solving ordinary differential equations with two-point conditions are investi-

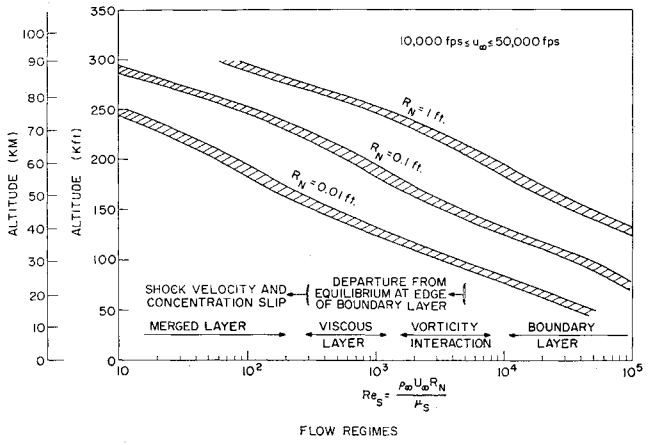

Fig. 1 Flow regimes.

gated. These methods of solution are much more satisfactory than previous initial value techniques with iteration of guessed boundary conditions.

The flow in the stagnation region of a blunt body has been classified into a number of regimes by Probstein,[2] and these results have been rearranged into Fig. 1. Also shown in this figure, as given by Inger,[3] is the value of the shock Reynolds number at which the Rankine-Hugoniot relations break down and the inviscid flow is no longer in equilibrium. As this figure shows, the boundary-layer theory can be employed only at the lower altitudes, but the appropriate altitude increases as the nose radius becomes larger. The present investigation will consider the regimes from boundary-layer flow through the viscous layer flow.

The thin, viscous shock-layer equations, as developed by Ho and Probstein,[4] and independently developed and simplified by Cheng,[5] are the ones considered in this study. These equations are the same as the first-order boundary-layer equations, except a normal momentum equation must be included. The difference between the boundary-layer theory and the thin-shock-layer theory is in the manner the boundary conditions are applied at the outer edge. For the shock layer, the Rankine-Hugoniot shock conditions are applied at a finite distance from the surface, which is determined by matching the appropriate velocity behind the shock wave. In the paper by Cheng,[5] modified Rankine-Hugoniot relations are employed, which take into account a shock transition zone, but the gas is assumed frozen across this region. With these modified Rankine-Hugoniot relations, the thin-shock-layer analysis can be extended into the merged layer regime, but this is not completely appropriate if one is interested in flows with finite chemical reactions. Another approach is to solve the flow throughout the viscous shock layer and shock transition zone, as has been done by Lee and Zierten.[6] This method is not physically correct, as the Navier-Stokes equations are invalid for the structure of a strong shock wave. The present investigation is restricted to the domains pertaining to the viscous layer, vorticity interaction, and boundary layer where chemical nonequilibrium effects are more important and shock slip effects can be neglected.

There have been a number of papers concerned with the viscous, thin-shock-layer theory at the stagnation point of a blunt body. A complete review of the viscous hypersonic blunt-body problem was made recently by Cheng.[7] Many of the papers have employed a perfect gas model, such as Refs. 4 and 8–14, or equilibrium air, such as Refs. 15–18. Also, there have been several papers[5,19–23] concerned with the viscous shock layer for a binary gas mixture with a finite chemical reaction rate. The papers by Stoddard[22] and Buckmaster[23] are even more restrictive, as the analytical solutions presented require a small degree of dissociation and negligible recombination rate. Also, most of these papers employ simplified thermodynamic and transport properties. The paper by Lee and Zierten[6] has employed the most complete chemistry; however, the species equations are decoupled from the other thin-shock-layer equations. This brief review is intended to show that a significant amount of work has been devoted to the understanding of the fluid dynamics of the viscous hypersonic blunt-body problem, but there is a need for solutions of this problem with realistic gas models. It is the intention of the present investigation to help provide these types of results.

2. Governing Equations

The general equations for a multicomponent chemically reacting gas mixture are given in Ref. 24 and these can be written for the shock layer in a manner similar to Cheng.[5] The resulting partial differential equations are the same as those employed in boundary-layer studies in Ref. 25, except the normal momentum equation

$$(dp/dy) + \kappa_c \rho u^2 = 0 \tag{1}$$

must be included. The governing equations are transformed by introducing new independent variables

$$\xi(x) = \int_0^x (\rho\mu)_r u_e r_b^{2i} dx, \quad \eta(x,y) = \frac{u_e r_b^i}{(2\xi)^{1/2}} \int_0^y \rho dy \tag{2a}$$

and new dependent variables

$$f' = u/u_e, \quad \theta = T/T_e \tag{2b}$$

The resulting equations are given in Ref. 25 with $\bar{e} = -1$ (see Eq. 5). For the case $\xi = 0$, which corresponds to a stagnation point or the tip of a sharp body, the equations become, for continuity,

$$(dV/d\eta) + f' = 0 \tag{3a}$$

for tangential momentum,

$$d/d\eta[l(df'/d\eta)] - V(df'/d\eta) - \beta[(\bar{M}_e\theta/\bar{M}\bar{e}) + (f')^2] = 0 \tag{3b}$$

for normal momentum

$$(dp/d\eta) + [\kappa_c u^2 (2\xi)^{1/2}/u_e r_b^i] = 0 \tag{3c}$$

for energy

$$\frac{1}{\bar{c}_p}\frac{d}{d\eta}\left(\frac{l\bar{c}_p}{Pr}\frac{d\theta}{d\eta}\right) - V\frac{d\theta}{d\eta} + \frac{u_e^2}{\bar{c}_p T_e}\left[l\left(\frac{df'}{d\eta}\right)^2 + \frac{\beta\bar{M}_e}{\bar{e}\bar{M}} f'\theta\right] + \sum_{i=1}^{NI} \frac{c_{pi} l}{\bar{c}_p Pr}\left(Le_i \frac{dc_i}{d\eta} + \sum_{\substack{k=1 \\ k\neq i}}^{NI} \Delta\bar{\bar{b}}_{ik}\frac{dc_k}{d\eta}\right)\frac{d\theta}{d\eta} - \frac{2\xi}{\bar{c}_p T_e u_e d\xi/dx}\sum_{i=1}^{NI} h_i\left(\frac{w_i}{\rho}\right) = 0 \tag{3d}$$

for species continuity

$$\frac{d}{d\eta}\left[\frac{l}{Pr}\left(Le_i\frac{dc_i}{d\eta} + \sum_{\substack{k=1 \\ k\neq i}}^{NI}\Delta\bar{\bar{b}}_{ik}\frac{dc_k}{d\eta}\right)\right] - V\frac{dc_i}{d\eta} + \frac{2\xi}{u_e d\xi/dx}\left(\frac{w_i}{\rho}\right) = 0 \tag{3e}$$

where

$$\beta = (2\xi/u_e)(du_e/d\xi)\,[\text{at stagnation point } \beta = 1/(1+j)]$$

$$\bar{e} = \rho_e u_e[(du_e/dx)/(dp/dx)]$$

$$Le_i = \sum_{\substack{j=1 \\ j\neq i}}^{NI}\frac{c_j}{M_j} \Bigg/ \sum_{\substack{j=1 \\ j\neq i}}^{NI}\frac{c_j}{M_j\mathcal{L}_{ij}}$$

$$\Delta\bar{\bar{b}}_{ik} = Le_i - \left[\frac{M_i}{\bar{M}}L_{ik} + \left(1 - \frac{M_i}{M_k}\right)\sum_{j=1}^{NI} L_{ij}c_j\right]$$

If the binary Lewis-Semenov numbers, $\mathcal{L}_{ij}$, are constant for all the species or if a trace species is being considered, the term $\Delta\bar{b}_{ik}$ is zero. In the previous equation, the pressure and thermal diffusion terms are neglected because of the boundary-layer assumption; and the force diffusion term is assumed zero. The equation of state also is required and is written as

$$\rho = \left(p_e \Big/ RT \sum_{i=1}^{NI} \frac{c_i}{M_i}\right) = \frac{p_e \bar{M}}{RT} \tag{4}$$

where it is assumed the gas consists of a mixture of chemically reacting perfect gases and the pressure change across the layer is neglected as a result of Eq. (3c). However, there is a variation of the rate of change of the tangential pressure gradient across the layer at the stagnation point, which can be determined from Eq. (3c). When the pressure is solved from Eq. (3c) and differentiated with respect to x, the following is obtained at the stagnation point:

$$e = \rho_s u_s \left(\frac{du_s/dx}{dp/dx}\right) = -\frac{1}{2\epsilon}\left\{\frac{(1-\epsilon)}{[1-\epsilon(1-1/s)]^2} + \frac{\int_\eta^{\eta_s}(f')^2 d\eta}{\{(1+j)Re_s\epsilon[s(1-\epsilon)+\epsilon]\}^{1/2}}\right\}^{-1} \tag{5}$$

where

$$s = (R_N/R_s)[1 + (\Delta/R_N)]$$

For the boundary-layer problem, the value of $\bar{e} = -1$ when the flow for the body streamline is used as the edge conditions.

The conditions at the surface and outer edge of the boundary layer determine the necessary boundary conditions for the foregoing equations. At the wall, it is assumed that the tangential velocity is zero and the surface temperature is specified. These conditions are expressed as

$$u(0) = 0,\ T(0) = T_b \tag{6a}$$

In addition, the boundary condition on the mass flux of a species "i" at the surface $(\rho_i v_i)_b$ is

$$(\rho_i v_i)_b = \dot{m}_i = (c_i \rho v)_b + (j_i)_b \tag{6b}$$

The mass flux of a species at the surface, $\dot{m}_i$, depends on the surface material and how it interacts with the gases in the boundary layer. In the present study, only the extreme case of a fully catalytic surface is considered. For a fully catalytic wall, the gas is assumed undissociated and unionized. The total mass flux at the surrace is zero for this case.

The flow at the edge of the shock layer is obtained from the Rankine-Hugoniot relations

$$p_s = p_\infty + \rho_\infty V_\infty^2(1 - v_s/V_\infty)$$
$$h_s = h_\infty + \tfrac{1}{2}V_\infty^2[1 - (v_s/V_\infty)^2] \tag{7}$$
$$T_s = \left(h_s - \sum_{i=1}^{NI} c_i \Delta h_i^F\right) \Big/ \sum_{i=1}^{NI} c_i c_{1i},\quad \frac{v_s}{V_\infty} = \frac{\rho_\infty}{\rho_s} = \frac{p_\infty T_s}{p_s T_\infty}$$

An iteration process is used to solve the preceding equations where, initially, (v_s/V_∞) is assumed zero and the denominator in Eq. (7) is taken equal to 7000. The mass fractions of species across the shock are taken constant. The use of the Rankine-Hugoniot relations (7) rather than the modified relations as employed by Cheng[5] will limit the applicability of the analysis to shock-layer Reynolds numbers greater than approximately 100. The boundary conditions at the outer edge of the shock layer are expressed as

$$V(\eta_e) = -\{\epsilon Re_s/(1+j)[s(1-\epsilon)+\epsilon]\}^{1/2} \tag{8a}$$

$$f'(\eta_e) = 1,\ \theta(\eta_e) = 1,\ c_i(\eta_e) = c_{ie} = c_{is} = c_{i\infty} \tag{8b}$$

For the shock-layer flow, the value of $\eta_e = \eta_s$ must be varied until condition (8a) is satisfied.

When the shock-layer Reynolds number becomes large, the solution of Eqs. (3) from the body to the shock is not necessary. In this case, the boundary-layer approach can be followed where the edge conditions are obtained from the inviscid flow at the surface where the air is assumed in chemical equilibrium. For the boundary-layer approach, the value of $\eta_e \approx 6$ and condition (8a) is not required.

3. Thermodynamic and Transport Properties and Chemical Kinetics

The thermodynamic properties of enthalpy and specific heat of the individual species (O_2, N_2, O, N, NO, NO^+) are obtained from tabulated values as given by Browne.[26-28] The thermodynamic and transport properties based on the air model employed in this paper have been determined for an equilibrium composition at a pressure of 1 atmosphere and temperatures up to 20,000°K. The present results for enthalpy have been compared with predictions of Predroditelev[29] and Hansen.[30] These authors are in close agreement except at temperatures around 4000°K. The present frozen specific heat at constant pressure has been compared to the results of Hansen. The present results for enthalpy and specific heat are in good agreement with the predictions of these authors except at temperatures above 10,000°K. This is expected, as the present gas model is valid only when there is a slight amount of ionization.

The viscosity and thermal conductivity of the gaseous mixture is calculated from Wilke's semiempirical relations (see pp. 24 and 258 of Ref. 24). The viscosities of the individual species are those given by Yun and Mason.[31] The viscosity of NO^+ is assumed equal to that of NO. The present frozen thermal conductivity and viscosity of equilibrium air at atmospheric pressure have been compared to results of Hansen[30] and Yos.[32] These properties are in reasonable agreement with the predictions of Yos when the temperature is less than 10,000°K.

The thermodynamic and transport properties employed in the shock-layer solution in this paper are more accurate than is indicated by the equilibrium properties. When the temperature behind the shock is very high, the predominant species are molecular oxygen and nitrogen which are included in the gas model with reasonable accuracy. The temperature decreases toward the body, and probably no significant amounts of ionized atomic and molecular species have time to be produced. Therefore, the present gas model is considered reasonable for the cases investigated in this paper.

The net mass rate of production of a chemical species per unit volume is obtained from the usual relations as given in Ref. 25. The following chemical reactions are used for the pure air gas model:

$$r = 1 \quad O_2 + M_1 \rightleftarrows 2O + M_1 \tag{9a}$$
$$2 \quad N_2 + M_2 \rightleftarrows 2N + M_2 \tag{9b}$$
$$3 \quad N_2 + N \rightleftarrows 2N + N \tag{9c}$$
$$4 \quad NO + M_3 \rightleftarrows N + O + M_3 \tag{9d}$$
$$5 \quad NO + O \rightleftarrows O_2 + N \tag{9e}$$
$$6 \quad N_2 + O \rightleftarrows NO + N \tag{9f}$$
$$7 \quad N + O \rightleftarrows NO^+ + e^- \tag{9g}$$

The forward reaction rates for the aforementioned reactions are expressed as

$$k_{f_r} = T_K^{C2_r} \exp(\ln C0_r - C1l_r \times 10^3/T_K)$$

where the backward rate is the same form as the forward, with the constants C replaced with D's. The values of these reaction-rate coefficients as obtained from Bortner[33] are given in Table 1. The corresponding third body efficiencies relative to argon are given in Table 2.

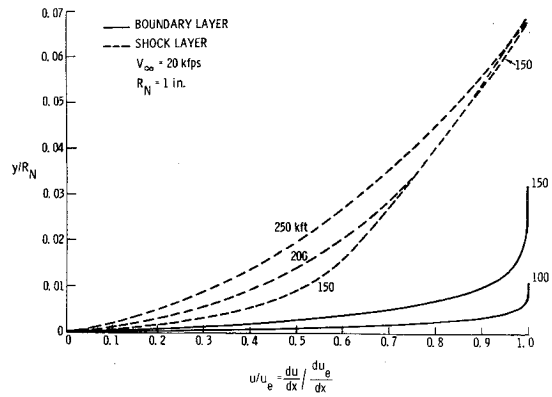

Fig. 2 Tangential velocity gradient across shock layer.

4. Method of Solution

From previous experience with initial value techniques and the resulting difficulties encountered, a finite difference method was initially chosen as the method of solution. The finite difference equations were made linear in the unknown variables and any coupling between the equations was eliminated. If coupling between the equations is allowed (this is required for the quasilinearization technique as defined by Bellman and Kulaba[34]), the resulting system of algebraic equations for a gas mixture with many chemical species requires an excessive amount of rapid-access computer storage. Therefore, the present scheme uncouples the conservation equations.

The governing Eqs. (3) are written in the following form:

$$(d^2W/d\eta^2) + \alpha_1(dW/d\eta) + \alpha_2 W + \alpha_3 = 0 \qquad (10)$$

where, for the tangential momentum equation, $W = f'$

$$\alpha_1 = (l' - V)/l, \quad \alpha_2 = -2\beta f'/l \qquad (11a,b)$$

$$\alpha_3 = -(\beta/l)[(\bar{M}_e/M)(\theta/\bar{e}) - (f')^2] \qquad (11c)$$

for the energy equation, $W = \theta$,

$$\alpha_1 = [\bar{c}' - \bar{c}_p(V + d + b)]/\bar{c} \qquad (12a)$$

$$\alpha_2 = \left\{\frac{\alpha\beta}{\bar{e}}\bar{c}_p\frac{\bar{M}_e}{\bar{M}}f' - \sum_{i=1}^{NI}\left[\bar{W}_i c_{1i} + \frac{eh_i}{T_e}\frac{\partial}{\partial\theta}\left(\frac{w_i}{\rho}\right)\right]\right\}\Big/\bar{c} \qquad (12b)$$

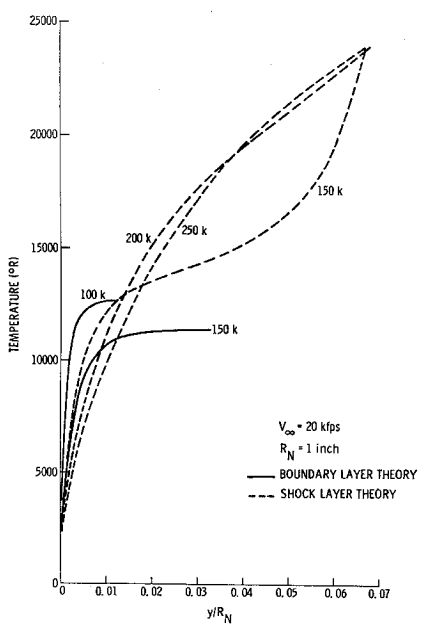

Fig. 3 Temperature across shock layer.

Table 1 Reaction rate coefficients

Reaction	CO(r)	C1(r)	C2(r)	D0(r)	D1(r)	D2(r)
r = 1	3.61×10^{18}	59.4	−1.0	3.01×10^{15}	0	−0.5
2	1.92×10^{17}	113.1	−0.5	1.09×10^{16}	0	−0.5
3	4.15×10^{22}	113.1	−1.5	2.32×10^{21}	0	−1.5
4	3.97×10^{20}	75.6	−1.5	1.01×10^{20}	0	−1.5
5	3.18×10^{9}	19.7	1.0	9.63×10^{11}	3.6	0.5
6	6.75×10^{13}	37.5	0	1.50×10^{13}	0	0
7	9.03×10^{9}	32.4	0.5	1.80×10^{19}	0	−1.0

$$\alpha_3 = \left\{\alpha l\bar{c}_p\left(\frac{\partial f'}{\partial\eta}\right)^2 - \frac{1}{T_e}\times \sum_{i=1}^{NI}\left[\bar{W}_i\Delta h_i^F - eh_i\theta\frac{\partial}{\partial\theta}\left(\frac{w_i}{\rho}\right)\right]\right\}\Big/\bar{c} \qquad (12c)$$

for the species equation, $W = c_i$ $(i = 1, 2, \ldots NI)$

$$\alpha_1 = [b_i' - V]/b_i, \quad \alpha_2 = -eW_i^1/b_i \qquad (13a,b)$$

$$\alpha_3 = (eW_i^0 + \bar{b}_i')/b_i \qquad (13c)$$

where

$$\frac{\partial}{\partial\theta}\left(\frac{w_i}{\rho}\right) = \frac{M_i}{\theta}\sum_{r=1}^{NR}(\beta_{ri} - \alpha_{ri})\times \left[\left(C2_r + \frac{C1_r}{T_K} - \alpha_r\right)L_{fr} - \left(D2_r + \frac{D1_r}{T_K} - \beta_r\right)L_{br}\right]$$

The other quantities introduced into the previous expressions are given below;

$$\alpha = u_e^2/(\bar{c}_p T_e), \quad \beta = 1/(1 + j)$$

$$\bar{e} = \rho_e u_e\frac{du_e/dx}{dp_e/dx} = \begin{cases} -1 \text{(boundary layer)} \\ \text{See Eq. (5) (shock layer)} \end{cases}$$

$$e = \frac{2\xi}{u_e d\xi/dx} = \begin{cases} 0 \text{ (tip of cone)} \\ \dfrac{1}{(1 + j)du_e/dx} \text{ (stagnation point)} \end{cases}$$

$$b_i = \frac{lLe_i}{Pr}, \quad \bar{b}_i = \frac{l}{Pr}\sum_{\substack{k=1 \\ k\neq i}}^{NI}\Delta\bar{b}_{ik}\frac{dc_k}{d\eta}$$

$$b = -\sum_{i=1}^{NI}\frac{c_{pi}\bar{b}_i}{\bar{c}_p}, \quad \frac{w_i}{\rho} = W_i^0 - W_i^1 c_i$$

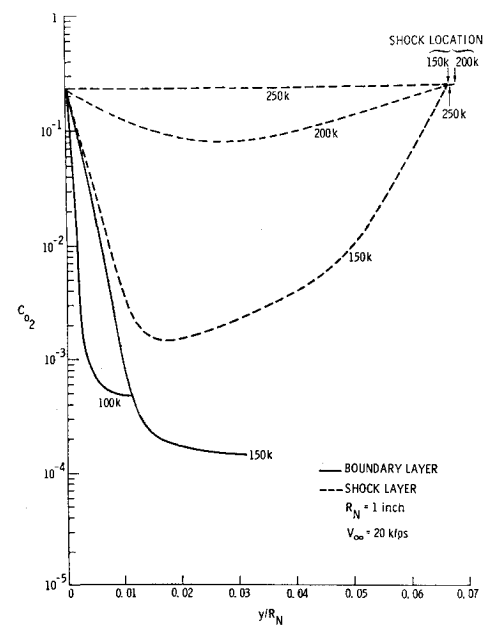

Fig. 4 Mass fraction of molecular oxygen across shock layer.

Table 2 $Z_{(j-NI)i}$, **third body efficiencies relative to Ar**

	$i = 1$ O_2	2 N_2	3 O	4 N	5 NO	6 NO^+
$(j - NI) = 1$ (e^-)	0	0	0	0	0	1
$= 2$ (M_1)	9	2	25	1	1	0
$= 3$ (M_2)	1	2.5	1	0	1	0
$= 4$ (M_3)	1	1	20	20	20	0

$$\bar{W}_i = e(w_i/\rho),\ \bar{c} = l\bar{c}_p/Pr$$

$$\frac{du_e}{dx} = \begin{cases} \dfrac{1}{R_N}\left[\dfrac{2(p_{e_s} - p_\infty)}{\rho_{e_s}}\right]^{1/2} & \text{(boundary layer)} \\ \dfrac{V_\infty}{R_N}\,[s(1-\epsilon)+\epsilon] & \text{(shock layer)} \end{cases}$$

$$d = -\sum_{i=1}^{NI} \frac{c_{pi}}{\bar{c}_p} b_i \frac{dc_i}{d\eta},\ (\ )' = \frac{d(\ )}{d\eta}$$

The ordinary differential equation (10) is written in finite-difference form, with the usual difference quotients involving three points. The resulting equations are linear algebraic equations and, with the boundary conditions, give a system of the tridiagonal form. An efficient method of solution† for computers is available. If the ordinary differential equation is nonlinear, then α_1, α_2, and α_3 must be approximated by assuming an initial distribution of the independent variable W. Then the solution can be obtained to give a new value of W. This procedure can be repeated until the assumed value of W is the same or nearly the same as the calculated value of W. For some problems it is necessary to weigh the assumed and calculated solution to obtain a new assumed solution for the next iteration.

For the iteration procedure to converge and to have a reasonable rate of convergence, several items have been found important in the method of solution. How the chemical production terms are written is very important. The linearization technique employed in Ref. 25 cannot be used in this case, since that procedure involves a Taylor's-series expansion of all of the species and the temperature. When this procedure is followed, all the species and energy equations would be coupled together. As indicated above, the production term is written as

$$w_i/\rho = W_i^0 - W_i^1 c_i \tag{14}$$

where, for a binary mixture of oxygen, the only reaction is Eq. (9a) and

$$W_0^0 = 2M_0 k_{f1}\bar{\rho}\gamma_{0_2}\gamma_{M_1},\ W_0^1 = k_{b1}\bar{\rho}^2\gamma_0\gamma_{M_1} \tag{15}$$

Table 3 Conditions for example investigated

Case	Altitude	Theory[a]	T_w (°K)	Re_s	p_e (psf)	T_e (°R)
A	100*K*	*BL*	1400	1.43×10^4	12772	12603
1	150*K*	*BL*	1000	1.54×10^3	1377	11330
2	150*K*	*SL*	1000	9.31×10^2	...	...
3	200*K*	*SL*	1000	1.38×10^2	...	...
B	250*K*	*SL*	1000	1.99×10^1	...	...

$V_\infty = 20$ kfps, $R_N = 1$ in } for all cases

[a] *BL* = boundary layer; *SL* = shock layer.

† This method apparently has been developed by several authors, but Bruce, Peaceman, Rachford, and Rice generally are given the credit in this country.[35] In Russia, this procedure is known as the "chasing" or double-sweep method, which was developed by Gelfund and Lokutsievski.[36]

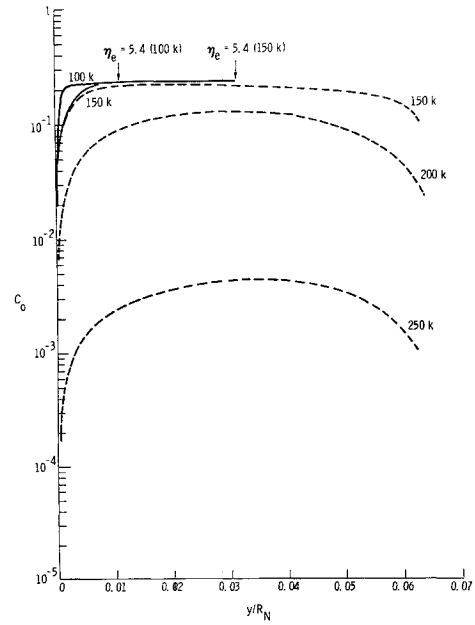

Fig. 5 Mass fraction of atomic oxygen across shock layer.

For the case of an air mixture, reactions 4, 5, 6, and 7 contribute to the chemical production term of atomic oxygen. In each reaction, either the forward or backward term involves the mass fraction of atomic oxygen and allows the chemical production term to be expressed as relation (14). Similar comments can be made about the production term for other species. For rapid convergence of the finite-difference solution, it is desirable that the terms W_i^0 and W_i^1 be as nearly constant as possible. For the case of oxygen, the value of W_0^0 is proportional to γ_{0_2} and, when the oxygen is highly dissociated, the value of γ_{0_2} changes rapidly for a small change in γ_0, since $\gamma_{0_2} = (1 - c_0)/M_{0_2}$. Therefore, it was found better to write the terms W_0^0 and W_0^1 for oxygen as

$$W_0^0 = 2M_0 k_{f1}\bar{\rho}\gamma_{M_1}(\gamma_{0_2} + \tfrac{1}{2}\gamma_0) = k_{f1}\bar{\rho}\gamma_{M_1} \tag{16a}$$

$$W_0^1 = k_{b1}\bar{\rho}^2\gamma_0\gamma_{M_1} + k_{f1}\bar{\rho}\gamma_{M_1} \tag{16b}$$

For the case of the air mixture, the terms W_i^0 and W_i^1 were expressed in a similar manner to relations (15). Then the

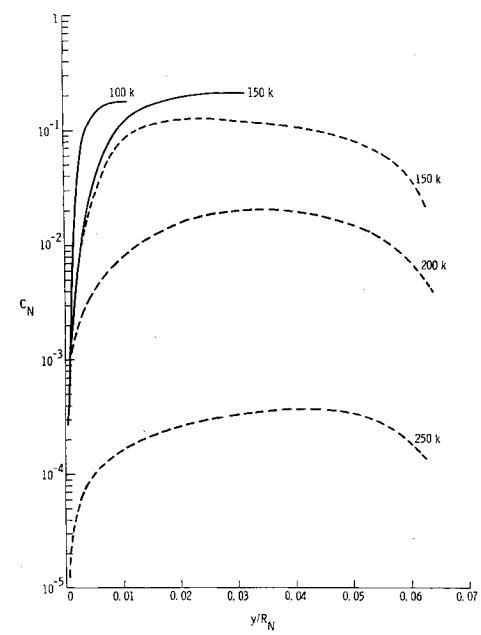

Fig. 6 Mass fraction of atomic nitrogen across shock layer.

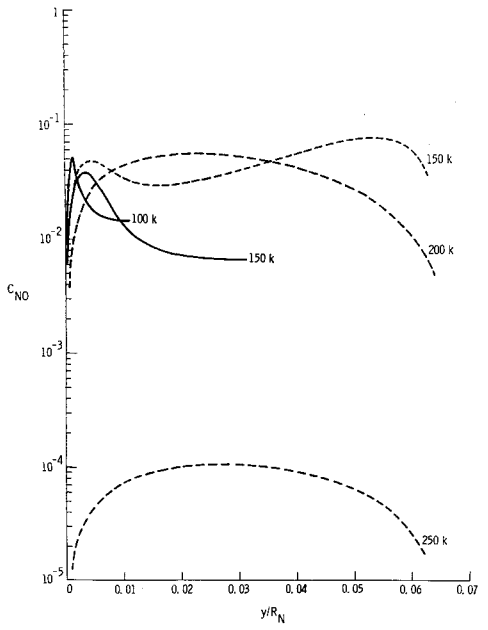

Fig. 7 Mass fraction of nitric oxide across shock layer.

W_i^0 and W_i^1 for atomic oxygen were modified by adding $M_0 k_{f1} \bar{\rho} \gamma_{M_1} \gamma_0$ and $k_{f1} \bar{\rho} \gamma_{M_1}$, respectively, to these terms, as has been done in relations (16).

When the conservation equations are uncoupled and the dependent variables are solved one at a time, the order in which the variables f', θ, and c_i's are solved must be chosen. The present investigation has shown that the species equations should be solved before the energy equation. The mass fraction of species obtained from the solution of the species equations are used in Eq. (14) to evaluate the chemical production term that is required in the energy equation. The terms W_i^0 and W_i^1 are not recalculated in Eq. (14). The transformed velocity V is obtained from the integration of Eq. (3a).

The method of nonlinear overrelaxation[37] also has been used to solve Eq. (10). An investigation was made for a binary gas of oxygen to compare the nonlinear overrelaxation method with the finite-difference procedure. It appears that the finite-difference procedure generally converges faster, as one would expect. For example, for a linear ordinary differential equation, the finite-difference procedure would give the solution directly, whereas the nonlinear overrelaxation method would still require an iteration procedure. The nonlinear overrelaxation method, however, probably will give convergent solutions for cases when the finite-difference method diverges.

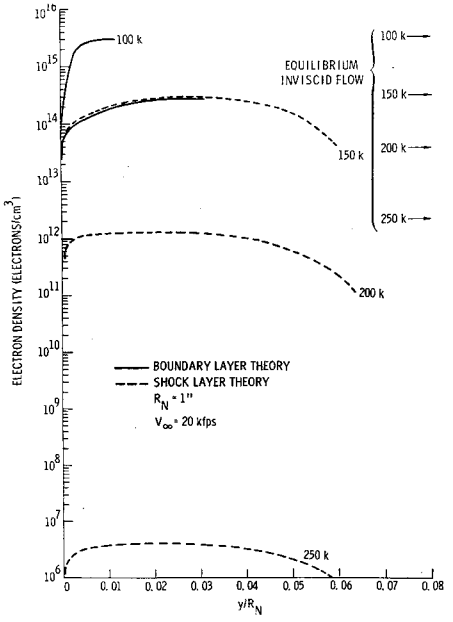

Fig. 8 Electron number density across shock layer.

5. Discussion of Results

In the AGARD seminar it was requested that two flight environments be investigated, which are called case A and case B, and the conditions are given in Table 3. When Fig. 1 is used, case A should correspond to a boundary-layer flow with equilibrium inviscid flow at the edge, whereas case B is in the merged layer regime. The computer program that solves the viscous shock layer also will solve the boundary-layer equations that are needed to investigate case A. Since the present viscous shock-layer solution uses the Rankine-Hugoniot relations, the resulting solutions cannot be expected to be completely valid for case B where shock slip effects are important. Three other cases also are investigated as indicated in Table 3. With the aid of Fig. 1, case 1 with boundary-layer theory should not be appropriate, whereas cases 2 and 3 with shock-layer theory should be a reasonable approach.

In the present solutions, the binary Lewis-Semenov numbers all have been assumed equal to 1.4. It also is assumed that the shock is concentric with the body, which makes $s = 1$. At the wall the gas is undissociated and unionized, which corresponds to a fully catalytic wall when the wall temperature is low.

The tangential velocity gradient at the stagnation point is given for the shock-layer solutions in Fig. 2. For the 150- and 200-kft altitude cases, there is a boundary-layer region. For the 250-kft case, a boundary layer cannot be readily identified. The tangential velocity gradient for the two boundary-layer cases also are presented. It should be noticed that the boundary-layer results are nondimensionalized by the tangential velocity gradient at the body surface, which is smaller than the tangential velocity gradient behind the shock that is used for the shock-layer results.

The temperatures across the shock layer as obtained from the boundary-layer and shock-layer theories are given in Fig. 3. The temperature is high behind the shock and decreases as the gas dissociates toward the body. This situation is especially true for the 150-kft case, but the gas has not reached equilibrium before the boundary layer is entered. The temperature close to the body surface is nearly the same for both the shock-layer and boundary-layer results for the 150-kft case. This figure indicates that a well-defined boundary layer with the inviscid edge flow in chemical equilibrium occurs at some altitude below 150 kft.

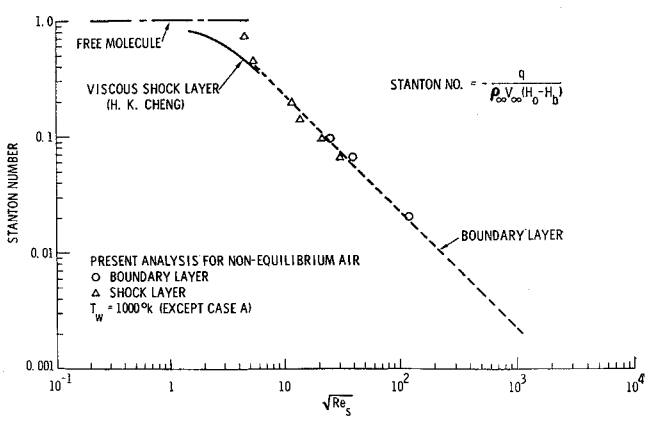

Fig. 9 Stanton number variation with Reynolds number.

The mass fractions of the various chemical species are given in Figs. 4–7. For the 250-kft case, the air is slightly dissociated, but for the other cases, there is an appreciable amount of dissociated species. The conditions corresponding to the edge of the boundary layer in the shock-layer solution at 150 kft indicate that the gas has not reached chemical equilibrium. Therefore, the assumption that the inviscid flow is in equilibrium for the 150-kft case is not correct. This agrees with the information presented in Fig. 1. The electron number density is given in Fig. 8, where the shock-layer and boundary-layer results are nearly the same for the 150-kft case. For the 250-kft case, there is only a slight amount of ionization.

The present results obtained for Stanton number are compared to various theories in Fig. 9. In this figure, additional results to the five cases given in Table 3 are presented to make the plot more complete. The free molecule and boundary-layer results were obtained from Ho and Probstein.[4] The free molecule results are for infinite Mach number and complete accommodation. The boundary-layer results are based on the work of Fay and Riddell,[38] and the enthalpy at the wall is taken as $0.025V_\infty^2$. The viscous shock-layer solution of Cheng[5] for a perfect gas also is given in this figure. The analysis of Cheng includes body- and shock-slip effects that have been neglected in the present analysis. The present results for small-shock Reynolds numbers are not valid, due to the neglect of the shock- and body-slip effects. The present results with a complete air model and with a catalytic wall are in reasonable agreement with the diatomic-air model results of Cheng[5] and Fay and Riddell.[38]

References

[1] Blottner, F. G., "Similar and Nonsimilar Solutions of the Nonequilibrium Laminar Boundary Layer," *AIAA Journal*, Vol. 1, No. 9, Sept. 1963, pp. 2156–2157.

[2] Probstein, R. F., "Shock-Wave and Flow Field Development in Hypersonic Re-entry," *ARS Journal*, Vol. 31, No. 2, Feb. 1961, p. 185.

[3] Inger, G. R., "Nonequilibrium Hypersonic Stagnation Flow with Arbitrary Surface Catalycity Including Low Reynolds Number Effects," *International Journal of Heat Mass Transfer*, Vol. 9, 1966, pp. 755–772.

[4] Ho, Hung-Ta and Probstein, R. F., "The Compressible Viscous Layer in Rarefied Hypersonic Flow," *Rarefied Gas Dynamics*, edited by L. Talbot, Academic Press, New York, 1961, pp. 525–552.

[5] Cheng, H. K., "The Blunt-Body Problem in Hypersonic Flow at Low Reynolds Number," IAS Paper 63-92, New York, Jan. 21–23, 1963; Rept. AF-1285-A-10, 1963, Cornell Aeronautical Lab.

[6] Lee, R. H. C. and Zierten, T. A., "Merged Layer Ionization in the Stagnation Region of the Blunt Body," *Proceedings of the 1967 Heat Transfer and Fluid Mechanics Institute*, edited by P. A. Libby, D. B. Olfe, and C. W. Van Atta, Stanford University Press, Stanford, Calif., 1967, pp. 452–468.

[7] Cheng, H. K., "Viscous Hypersonic Blunt-Body Problems and the Newtonian Theory," *Fundamental Phenomena in Hypersonic Flow*, edited by J. G. Hall, Cornell University Press, Ithaca, N.Y., 1966.

[8] Cheng, H. K., "Hypersonic Shock-Layer Theory of the Stagnation Region at Low Reynolds Number," *Proceedings of the 1961 Heat Transfer and Fluid Mechanics Institute*, Stanford University Press, Stanford, Calif., 1961, pp. 161–175.

[9] Kao, H. C., "Hypersonic Viscous Flow near the Stagnation Streamline of a Blunt Body: II. Third Order Boundary-Layer Theory and Comparison with Other Methods," *AIAA Journal*, Vol. 2, No. 11, Nov. 1964, pp. 1898–1906.

[10] Bush, W. B., "On the Viscous Hypersonic Blunt-Body Problem," *Journal of Fluid Mechanics*, Vol. 20, No. 3, Nov. 1964, pp. 353–367.

[11] Chen, S. Y., Aroesty, J., and Mobley, R., "The Hypersonic Viscous Shock Layer With Mass Transfer," *International Journal of Heat and Mass Transfer*, Vol. 10, Sept. 1967, pp. 1143–1158.

[12] Levinsky, E. S. and Yoshihara, H., "Rarefied Hypersonic Flow Over a Sphere," *Hypersonic Flow Research*, edited by F. R. Riddell, Academic Press, New York, 1962, pp. 81–106.

[13] Chen, S. Y., Baron, J., and Mobley, R., "Stagnation Region Gas Injection in Low Reynolds Number Hypersonic Flow," *Proceedings of the 1967 Heat Transfer and Fluid Mechanics Institute*, edited by P. A. Libby, D. B. Olfe, and C. W. Van Atta, Stanford University Press, Stanford, Calif., June 1967, pp. 34–57.

[14] Cheng, H. K. and Chang, A. L., "Stagnation Region in Rarefied High Mach Number Flow," *AIAA Journal*, Vol. 1, No. 1, Jan. 1963, pp. 231–233.

[15] Howe, J. T. and Viegas, J. R., "Solutions of the Ionized Radiating Shock Layer, Including Reabsorption and Foreign Species Effects, and Stagnation Region Heat Transfer," TR R-159, 1963, NASA.

[16] Edelman, R. and Hoffman, J., "Viscous Hypersonic Flow in the Vicinity of the Stagnation Point of Axisymmetric Blunt Bodies—Calculations and Results for Equilibrium Air," TR 498, May 1965, General Applied Science Lab. Inc., Westbury, N.Y.

[17] Goldberg, L., "The Structure of the Viscous Hypersonic Shock Layer," TIS-R65SD50, Dec. 1965, General Electric, Philadelphia, Pa.

[18] Hoshizaki, H., Neice, S., and Chen, K. K., "Stagnation Point Heat Transfer Rates at Low Reynolds Numbers," IAS Paper 60-68, June 1960.

[19] Chung, P. M., "Hypersonic Viscous Shock Layer of Nonequilibrium Dissociated Gas," TR R-109, 1961, NASA.

[20] Shih, W. C. L. and Krupp, R. S., "Viscous Nonequilibrium Blunt-Body Flow," *AIAA Journal*, Vol. 5, No. 1, Jan. 1967, pp. 16–25.

[21] Inger, G. R., "Nonequilibrium Hypersonic Stagnation Flow at Low Reynolds Numbers," SSD-TDR-64-118, Sept. 1964, Aerospace Corp., Inglewood, Calif.

[22] Stoddard, F. J., "Closed-Form Solutions for the Hypersonic Viscous Shock Layer with Finite-rate Chemistry," *Proceedings of the 1963 Heat Transfer and Fluid Mechanics Institute*, Stanford University Press, Calif., 1963, pp. 120–141.

[23] Buckmaster, J. D., "The Effects of Ambient Dissociation on Frozen Hypersonic Stagnation Flow," AEDC-TDR-64-142, June 1964, Cornell Aeronautical Lab., Buffalo, N.Y.

[24] Bird, R. B., Stewart, W. E., and Lightfoot, E. N., *Transport Phenomena*, Wiley, New York, 1960.

[25] Blottner, F. G., "Nonequilibrium Laminar Boundary Layer Flow of Ionized Air," *AIAA Journal*, Vol. 2, No. 11, Nov. 1964, pp. 1921–1927.

[26] Brown, W. G., "Thermodynamic Properties of Some Atoms and Atomic Ions," and "Thermodynamic Properties of Some Diatomic and Linear Polyatomic Molecules," MSD Engineering Physics TM 2 and 3, General Electric Co., Philadelphia, Pa.

[27] Browne, W. G., "Thermodynamic Properties of Some Ablation Products from Plastic Heat Shields in Air," MSD Aerospace Physics Memo 11, March 15, 1964, General Electric Co., Philadelphia, Pa.

[28] Browne, W. G., "Thermodynamic Properties of Some Diatoms and Diatomic Ions at High Temperature," and "Thermodynamic Properties of the Species CN, C_2, C_3, C_2N_2, and C^-," MSD Advanced Aerospace Physics TM 8 and 9, May 14, 1962, General Electric Co., Philadelphia, Pa.

[29] Predroditelev, A. S. et al., "Tables of Thermodynamic Functions of Air," translated and published by Associated Technical Services Inc., 1962, Glen Ridge, N.J.

[30] Hansen, C. F., "Approximations for the Thermodynamic and Transport Properties of High-Temperature Air," TN 4150, March 1958, NACA.

[31] Yun, K. S. and Mason, E. A., "Collision Integrals for the Transport Properties of Dissociating Air at High Temperatures," *Physics of Fluids*, Vol. 5, No. 4, 1962, pp. 380–386.

[32] Yos, Jerrold M., "Transport Properties of Nitrogen, Hydrogen, Oxygen, and Air to 30,000°K," RAD-TM-63-7, March 1963, Avco Corp., Wilmington, Mass.

[33] Bortner, M. H., "Suggested Standard Chemical Kinetics for Flow Field Calculations—A Consensus Opinion," *AMRC Proceedings*, Vol. 14, Part 1, 1966.

[34] Bellman, R. E. and Kulaba, R. E., *Quasilinearization and Nonlinear Boundary-Value Problems*, American Elsevier, New York, 1965.
[35] Richtmyer, R. D., *Difference Methods of Initial-Value Problems*, Interscience, New York, 1957, pp. 101–104.
[36] Godunov, S. K. and Ryabenki, V. S., *Theory of Difference Schemes*, North-Holland, Amsterdam, 1964.
[37] Ames, W. F., *Nonlinear Partial Differential Equations in Engineering*, Academic Press, New York, 1965.
[38] Fay, J. A. and Riddell, F. R., "Theory of Stagnation Point Heat Transfer in Dissociated Air," *Journal of the Aeronautical Sciences*, Vol. 25, No. 2, Feb. 1958, pp. 73–85.

DECEMBER 1969 AIAA JOURNAL VOL. 7, NO. 12

An Experimental Study of Fuel Droplet Ignition

BERNARD J. WOOD* AND WILLIS A. ROSSER JR.†
Stanford Research Institute, Menlo Park, Calif.

By means of photographic techniques, the size histories, ignition lags, and loci of ignition of small (from 100 to 300 μ in diameter), single, freely falling fuel droplets suddenly exposed to a hot, oxidizing atmosphere in a furnace were determined as a function of initial droplet size, oxidizer temperature, fuel composition, and droplet spacing. The results show that ignition lag depends significantly on the temperature of the atmosphere, on the droplet-droplet spacing, and on the chemical nature of the fuel, but it appears to be only weakly affected by the oxygen concentration in the oxidizer. The ignition lag seems to be independent of the initial droplet size if the droplets are large enough to ignite. This characteristic insures that droplets with initial diameters smaller than a characteristic value will not ignite during their lifetimes. In spite of the complexity of the ignition process, the experimental results give qualitative support to theoretical models representing approximations to the physical situation of a spontaneously igniting fuel droplet.

I. Introduction

EXTENSIVE studies[1,2] of the combustion characteristic of single droplets have contributed to a satisfactory analytical theory of steady-state droplet burning. The ignition process, a transition from a state in which the rate of chemical reaction is small to one in which the rate is large and is associated with a visible flame, is considerably more complex. Recently, the results of theoretical studies of droplet ignition and extinction, based on the model of a spherical droplet in a hot, gaseous environment, have been published.[3–5] Experimental studies, however, are essential as a firm empirical basis for the development and refinement of a satisfactory analytical theory of droplet ignition. The work described in this paper was undertaken with this specific objective in mind.

II. Experimental Studies

A. Approach

To understand the process of droplet ignition, certain parameters and their mutual dependence must be determined quantitatively. For a specific fuel of known thermodynamic and transport properties and a specific oxidizer temperature, we must know the rate of vaporization preceding ignition, the size of the droplet at ignition, and the duration of the ignition lag. Experiments on these variables have been carried out by many investigators using a variety of techniques.[1] In general, however, those who were able to observe the ignition behavior of individual droplets employed large drops [diameter (D) > 1000 μ] suspended on fibers; those who employed small, unsupported droplets depended on average mass or diameter changes and time extrapolations to obtain vaporization rates and ignition lags.

Our approach was to attempt direct and simultaneous measurement of the rate of vaporization, the diameter, and the ignition lag of small ($D \sim 100$ μ), freely falling droplets suddenly exposed to a hot oxidizing atmosphere, and to determine the effect on these parameters of droplet initial diameter and oxidizer composition and temperature.

B. Techniques

1. Measurement of preignition and postignition droplet vaporization rates

A photographic technique employing dark-field illumination was adapted to follow a liquid-fuel droplet along a free-fall trajectory in a heated furnace. The device, shown schematically in Fig. 1, consisted essentially of a camera, with a sufficiently long bellows to give 10 × magnification, looking through a furnace equipped with quartz windows into a dark-field condenser. The condenser collected light from a Strobotac‡ and focused it in a hollow cone at a point near the vertical axis of the furnace. Light diverging from this focal point fell outside the aperture of the camera lens, unless a spherical transparent droplet was situated in the cone. In that case, the droplet acted as a secondary lens that focused an image of the condenser into the field of view of the camera. The film recorded a bright ring with a diameter proportional to the focal length (and therefore the diameter) of the droplet. The constant of proportionality was determined empirically using glass spheres of known size fused on the ends of fine fibers in addition to freely falling liquid droplets sized by a standard replication technique.[6]

A monodisperse stream of droplets was produced by means of a resonant reed atomizer[7] driven at 60 cps. This device

Received November 15, 1968; revision received June 23, 1969. Work supported by U.S. Army Edgewood Arsenal under Contract DA-18-035-AMC-122(A). Much of the experimental work in this study was carried out by R. C. Smith.

* Chemist, Surface Physics and Chemistry Program. Associate Fellow AIAA.
† Senior Chemist, Surface Physics and Chemistry Program; now Principal Research Scientist, Avco Everett Research Laboratory, Everett, Mass.

‡ Model 1531-A, General Radio Corp., Cambridge, Mass.